Journal of Fusion Energy, Vol. 26, Nos. 1/2, June 2007 (© 2006)
DOI: 10.1007/s10894-006-9045-2

Spectroscopic Flow and Ion Temperature Studies of a Large *s* FRC

C. D. Cothran,[1,*] J. Fung,[1] M. R. Brown,[1] M. J. Schaffer,[2] and E. Belova[3]

The Swarthmore Spheromak Experiment (SSX) produces a large *s* FRC by merging counter-helicity spheromaks within a cylindrical flux conserver. Past results have shown that the toroidal fields in each spheromak do not annihilate even after the poloidal flux appears to have completely reconnected. This would suggest a radially directed current density at the mid-plane, and therefore a radially sheared azimuthal component of $J \times B$. In contrast, fast high resolution spectroscopic measurements indicate that flow at the midplane is small ($u < < v_A$) and there is little shear.

KEY WORDS: Magnetic confinement; field reversed configuration; spheromak merging.

The field reversed configuration (FRC) offers many attractive features for fusion reactor design. It is a $\beta \approx 1$, axisymmetric, compact toroidal (CT) magnetic confinement configuration with closed, purely poloidal field lines [1]. Because of its topology and high β, a number of engineering problems are mitigated and direct power conversion is possible, making it very well suited for advanced fuel reactor designs. The translatability makes the FRC attractive for alternative pulsed concepts such as magnetized target fusion [2].

The FRC is traditionally formed by a reversed theta-pinch. This technique typically produces an FRC characterized by a small value for the parameter *s*, roughly a measure of the number of ion gyroradii within the FRC minor radius, and large elongation $E = L/2R$, where L is the axial length and R the radius of the separatrix. These FRCs show remarkable resilience despite their highly dynamic formation process, and have lifetimes much greater than the characteristic Alfvén time.

Kinetic effects are thought to be responsible for the observed stability of small *s*, prolate (large *E*) FRCs. Experimentally, FRCs satisfying $s/E < 0.3$ are found to be stable. Recent numerical work is closing in on an understanding of this empirical boundary. Hybrid two-fluid simulations [3] have shown scaling in s/E of the linear tilt growth rate; furthermore, this growth rate is reduced primarily due to finite Larmor radius (FLR) effects, while the Hall effect determines the tilt mode structure and rotation. Nonlinear extension of these results show saturation of the tilt mode for small *s* [3].

However, an FRC reactor will require large values of *s* to have a sufficiently long energy confinement time. The experimentally determined stability boundary then would require a reactor design with impractically large *E*. At large *s*, kinetic effects diminish, and the stability of the FRC is determined by magnetohydrodynamics (MHD). Unfortunately, the tilt mode of the FRC is unstable in any generic

[1] Department of Physics and Astronomy, Swarthmore College, Swarthmore, PA, 19081, USA.
[2] General Atomics85608, San Diego, CA, 92186, USA.
[3] Plasma Physics Laboratory, Princeton University, Princeton, NJ, 08543, USA.
* To whom correspondence should be addressed: E-mail: ccothra1@swarthmore.edu

MHD analysis. Nonlinear studies, profile effects, field shaping, and rotation have all been examined; some reductions in the tilt growth is observed, but stability is still not obtained in the MHD limit [4]. One notable exception is the case of an oblate FRC, for which tilt stabilization by a close-fitting conducting shell was found [5].

The reversed theta pinch formation technique is unlikely to provide enough flux for an FRC reactor, so other formation methods have been investigated. The FRC has also been formed by rotating magnetic field [6, 7]. The counter-helicity spheromak merging technique for FRC formation was developed by Ono [8] in the TS-3 device at the University of Tokyo. This method has the advantage of producing relatively large s FRCs, and the energy of the toroidal field in the initial spheromaks is converted to ion energy (thermal and fluid velocity) during the merging process. The FRCs produced at TS-3, and now on the larger TS-4 device, are oblate, large s, and grossly stable, but are linked by a center conducting column on the geometric axis.

The Swarthmore Spheromak Experiment (SSX) has adopted the counter-helicity spheromak merging FRC formation technique to study modestly prolate FRCs in the MHD limit [9]. SSX uses opposing coaxial magnetized plasma guns to produce spheromaks at either end of a cylindrical volume bounded by a thin shell copper flux conserver, as indicated in Figure 1. The flux conserver has a length $L = 63$ cm and radius $R = 20$ cm, making the elongation $L/2R = 1.5$ which is unstable to the ideal MHD tilt. Note that there is no center conductor on the geometric axis; SSX produces true compact toroidal plasmas.

The gun flux can be adjusted, but typical SSX operation uses $\approx$1 mWb. The toroidal fields of the two spheromaks are always antiparallel. Changing the polarity of the gun flux reverses the direction of the poloidal field in the spheromaks; the gun flux polarity thus determines the sign of helicity (i.e., the handedness) of the spheromak produced. SSX spheromaks typically have about 3–4 mWb flux. Typical electron density is $\approx 1 \times 10^{15}/\text{cm}^3$, electron and ion temperatures are 10–30 eV, and $s \approx 8$ for the counter-helicity merging experiments reported here. These plasmas typically last about 100μs.

When the two guns are balanced to form spheromaks with equal but opposite (sign) helicity, an FRC (zero helicity) can be formed. Both the toroidal and poloidal fields of the original spheromaks are anti-parallel at the midplane, which is optimal for the magnetic reconnection which is necessary for the spheromaks to merge.

The toroidal current ($\approx$20–30 kA) in the initial spheromaks for counter-helicity merging are parallel, and therefore are grossly attractive. A pair of coils at the midplane produce a vacuum field that was originally intended to regulate the merging process. The flux surfaces shown in Figure 1 (for illustrative purposes only) correspond to an equilibrium for which only half the poloidal flux has reconnected and the magnetic axes of the two spheromaks remain. A figure-eight separatrix marks the boundary of the common (reconnected) flux and the private flux associated with each magnetic axis. The opposing

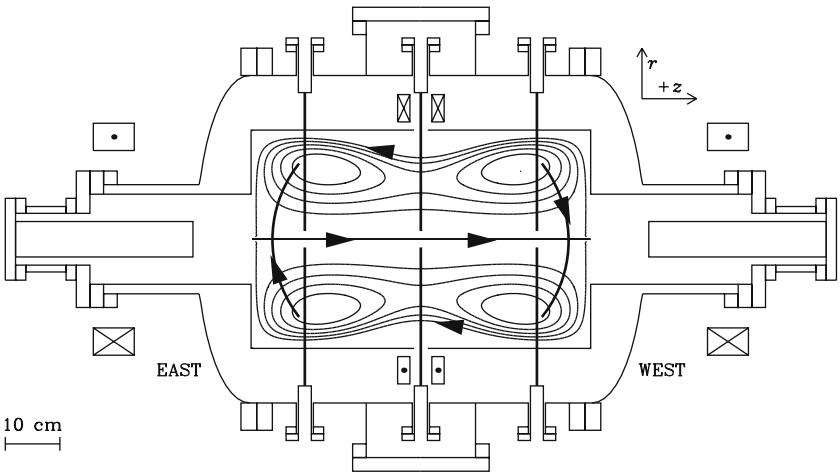

Fig. 1. The Swarthmore Spheromak Experiment (SSX) as configured for counter-helicity spheromak merging experiments, and flux surfaces for a Grad–Shafronov equilibrium for incomplete poloidal flux reconnection.

toroidal fields remaining at these axes have been drawn in. This equilibrium is a numerical solution computed using the EQLFE Grad–Shafronov solver [10] developed specifically to treat $r = 0$ correctly for CT equilibria.

Previous SSX results are reviewed below. Recently, a high resolution, fast time response ion Doppler spectroscopy (IDS) diagnostic [11] has been used for ion temperature and flow profile studies. This IDS instrument uses an echelle grating and multi-anode photomultiplier tube to achieve high resolution, fast time response, and large throughput. The shape of the CIII 229.687 nm emission line is monitored with $\approx$ 1μs time resolution throughout a spheromak merging experiment. The dispersion across the 1 mm wide channels of the PMT (currently 12 of 32 total channels are in use) is 0.0085 nm/mm for this line, giving an instrument temperature of 3.4 eV (for C ions). The systematic error in the velocity measurement due to the absolute wavelength calibration is better than ± 5 km/s. Only one view chord is analyzed at a time; 10 view chords evenly spaced in impact parameter from 0.2 cm (nearly a diameter) to 19 cm (not quite tangential to the flux conserver radius) are used for profile measurements.

Figure 2 shows the global magnetic structure measured after the spheromak merging process is complete. These internal measurements are obtained with linear probes inserted radially into the plasma volume at four toroidal positions and at three axial positions designated "east," midplane, and "west." Each linear probe measures all three field components at eight locations along its length (the spatial resolution is 2.5 cm). Figure 3 indicates the $m = 0$ (toroidally averaged) B_z profile at each axial probe position.

The time history of the poloidal flux (not shown; see [9] for details) indicates that the two spheromaks reconnect over approximately a 20–30μs time interval which ends by $t \approx 50$–60μs (pulsed power is applied to the guns at $t \equiv 0$). The IDS temperature measurements for a view chord along a diameter at the midplane (Fig. 4) indicates no dramatic ion heating during reconnection. By $t \approx 80$μs, the configuration is grossly distorted by tilt motion. Mode analysis shows that the inverse growth rate of the toroidal $m = 1$ mode is 6–8 Alfvén times (Fig. 5).

Contrary to expectation, the toroidal field of the two spheromaks clearly remain at each end of the configuration even after completion of the poloidal flux reconnection. The B_z profile at each end is consistent with the presence of the toroidal field: the zero-crossing of B_z occurs at approximately the location ($r \approx 12.5$ cm) that the simple zero-β Bessel function spheromak solution would predict. Similarly, the zero-crossing for B_z at the midplane (where there is no toroidal field) is consistent with the location ($r \approx 14$ cm) expected for the simple one-dimensional pressure balance of a $\beta = 1$ FRC. The midplane pressure balance condition also predicts a sensible total temperature of about 30 eV, based on

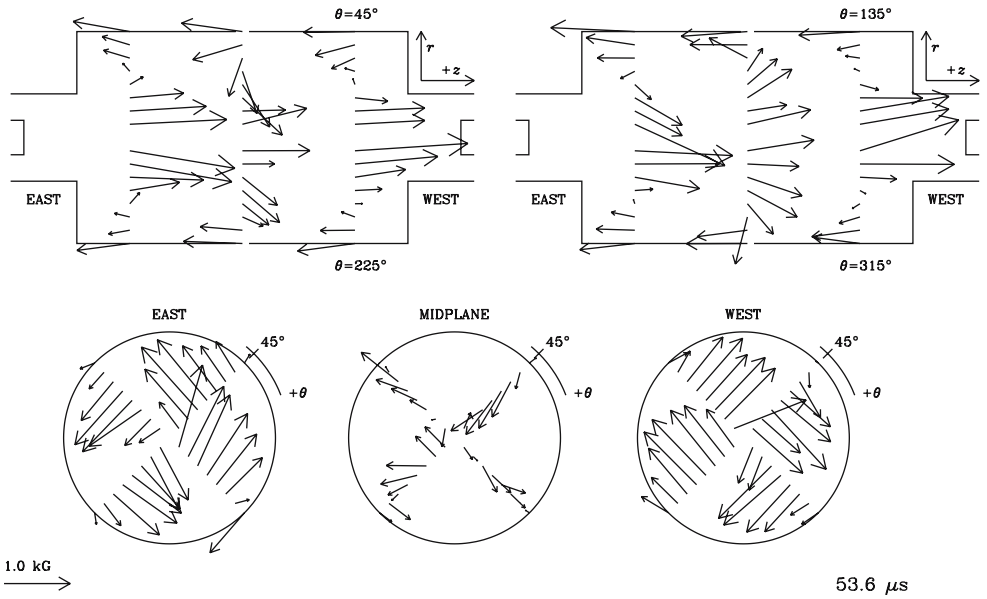

Fig. 2. Global magnetic structure. Five views of the data are shown: two orthogonal *rz* projections (top row) and three *r*θ projections (bottom row) at $t = 53.6\,\mu$s. The scale of 1 kG is indicated bottom left.

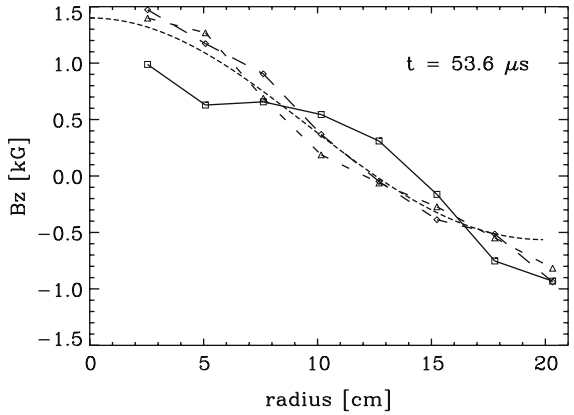

Fig. 3. Toroidally averaged B_z radial profile for the east, midplane, and west probe positions (diamond, square, and triangle plotting symbols, respectively). The force-free spheromak Bessel model (dotted) compares favorably to the east and west data. The field null at $r_0 \approx 14$ cm for the midplane data is consistent with the simple FRC prediction $r_0 = R_s/\sqrt{2}$.

the line-average electron density measured by interferometry.

Due to the poor axial resolution, it is not clear whether the toroidal fields (Fig. 2) are located in private flux regions, as in Figure 1. Since the poloidal flux measured at the ends is about the same as is measured at the middle, it appears that there is only one magnetic axis. If there are private flux regions, the configuration depicted in Figure 1 is perhaps more accurately described as a doublet-CT rather than an FRC. The net toroidal field, however, is nearly zero. A similar, but much smaller (compared to the poloidal field) axially-antisymmetric toroidal

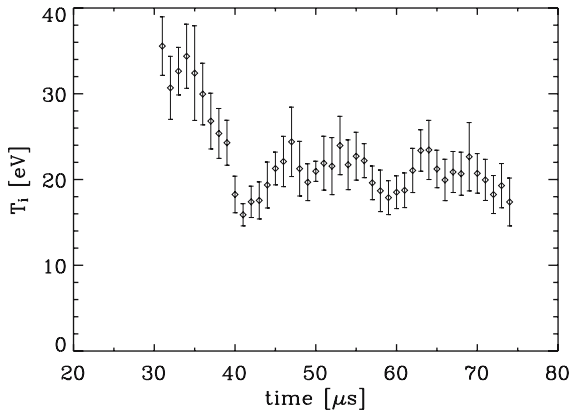

Fig. 4. Ion temperature averaged over 10 merging experiments. The IDS view chord for this measurement is along a diameter at the midplane. Large temperatures prior to $t = 40$ μs are likely due to the gun discharge, while the marginal $\approx$10 eV increase after $t = 40\mu$s may be due to reconnection.

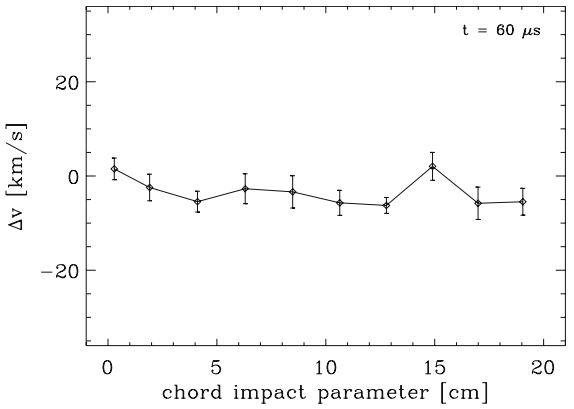

Fig. 5. Chord-averaged ion flow as a function of chord impact parameter after spheromak merging is complete. For comparison, the Alfvén velocity is $\approx$ 100 km/s.

field structure has been observed in translating theta-pinch formed FRCs [7]. A small net toroidal field has also been observed in FRCs [12] resulting in a high β configuration with properties similar to a spherical-tokamak (ST).

To support the anti-parallel toroidal fields at either end of the configuration, a radial current density must be present at the midplane. Since this current density crosses the poloidal field, there must be a toroidal $J \times B$ torque. Furthermore, since the poloidal field reverses, this torque is sheared radially. This torque must be balanced, either inertially or by viscous damping of a radially sheared toroidal flow. Significant midplane sheared flow is therefore expected, but not observed in the IDS measurements illustrated in Figure 4. These data are averaged over $\approx$10 shots at each chord. Large flow velocities up to ± 40 km/s observed intermittently during a single shot, however, do not survive this averaging.

Milroy [13] found that the Hall effect could generate exactly this pattern of toroidal field as well as toroidal flows in a simulation of FRC formation by the reversed theta pinch method. More recently, such toroidal fields were found to arise spontaneously in a nonlinear 3D hybrid, paricle-in-cell simulation [14] and were associated with a substantial decrease in the tilt growth rate. The TS-3 and TS-4 experiments have observed axially antisymmetric toroidal fields as well as a small sheared toroidal flow. Interestingly, this flow profile changed when the experiment was performed such that the polarity of the toroidal fields reversed with respect to the poloidal field [15].

In summary, SSX counter-helicity spheromak merging experiments have explored a large s FRC. Although the net toroidal flux is zero, this FRC has

the unusual feature of a strong axially-antisymmetric pattern of toroidal field (comparable to the poloidal field). The radial profile of B_z is consistent with a spheromak-like structure at either end and an FRC-like structure at the midplane. The toroidal fields suggest a strong radially sheared toroidal component of $J \times B$ at the midplane, but IDS measurements show no significant flow.

ACKNOWLEDGMENTS

This work was supported by grants from the Department of Energy and the National Science Foundation.

REFERENCES

1. M. Tuszewski, *Nucl. Fusion*, **28**, 2033 (1988)
2. T. Intrator, *et al.*, *Phys. Plasmas*, **11**, 2580 (2004)
3. E. Belova, R. C. Davidson, H. Ji, and M. Yamada, *Phys. Plasmas*, **10**, 2361 (2003)
4. R. D. Milroy, D. C. Barnes, R. C. Bishop, and R. B. Webster, *Phys. Fluids B: Plasma Phys.*, **1**, 1225 (1989)
5. E. Belova, S. C. Jardin, H. Ji, M. Yamada, and R. Kulsrud, *Phys. Plasmas*, **8**, 1267 (2001)
6. J. T. Slough, and K. E. Miller, *Phys. Rev. Lett.*, **85**, 1444 (2000)
7. H. Y. Guo, A. L. Hoffman, K. E. Miller, and L. C. Steinhauer, *Phys. Rev. Lett.*, **92**, 245001 (2004)
8 Y. Ono, A. Morita, T. Itagaki, and M. Katsurai, in *Plasma Physics and Controlled Nuclear Fusion Research* (IAEA, Vienna, 1993), vol. 2, p. 619
9. C. D. Cothran, A. Falk, A. Fefferman, M. Landreman, M. R. Brown, and M. J. Schaffer, *Phys. Plasmas*, **10**, 1748 (2003)
10. J. A. Leuer, M. J. Schaffer, P. B. Parks, and M. R. Brown, *Bull. Amer. Phys. Soc.*, **47**, 275 (2002)
11. C. D. Cothran, J. Fung, M. R. Brown, and M. J. Schaffer, *Fast high resolution echelle spectroscopy of a laboratory plasma*, submitted to *Rev. Sci. Instrum*
12. H. Y. Guo, A. L. Hoffman, L. C. Steinhauer, and K. E. Miller, *Phys. Rev. Lett.*, **95**, 175001 (2005)
13. R. D. Milroy, and J. U. Brackbill, *Phys. Fluids*, **29**, 1184 (1986)
14. Y. A. Omelchenko, M. J. Schaffer, and P. B. Parks, *Phys. Plasmas*, **8**, 4463 (2001)
15. Y. Ono, T. Matsuyama, K. Umeda, and E. Kawamori, *Nucl. Fusion*, **43**, 649 (2003)